Electronic Supplementary Material (ESI) for Physical Chemistry Chemical Physics.

Electronic Supplementary Information

Towards an atomistic understanding of polymorphism in molecular solids

Arturo Sauza-de la Vega, Leonardo J. Duarte, Arnaldo F. Silva, Jonathan M. Skelton,

Tomás Rocha-Rinza and Paul L. A. Popelier

	ΔE [kJ mol^{-1} molec^{-1} [a]]					
	This work			Ref. 7		
XC	$\Delta E(\alpha-\beta)$	$\Delta E(\gamma-\beta)$	**Ordering**	$\Delta E(\alpha-\beta)$	$\Delta E(\gamma-\beta)$	**Ordering**
PBE	-2.91	-1.72	$\alpha < \gamma < \beta$	-	-	
PBE0	2.38	-7.19	$\gamma < \beta < \alpha$	-	-	
B3LYP	0.65	-5.88	$\gamma < \beta < \alpha$	-	-	
PBE-D2	-0.40	0.17	$\alpha < \beta < \gamma$	-0.53	-0.59	$\gamma < \alpha < \beta$
PBE-D3	-0.64	-0.54	$\alpha < \gamma < \beta$	-	-	
PBE-TS	1.41	0.11	$\beta < \gamma < \alpha$	1.71	-0.42	$\gamma < \beta < \alpha$

[a] It is useful to clear up a potential confusion about the appearance of “per mole” alongside “per molecule”. An alternative unit often used is “electronvolts per molecule” or “eV molec^{-1}”. The substitution of the energy unit eV by the common energy unit “kJmol^{-1}“ is perhaps confusing in this context. The default interpretation of “kJmol^{-1}“ ought to be "kJ per mole of molecules". So the "per molecule" (i.e. “molec^{-1}”) appears redundant. However, leaving it out may lead to ambiguity when discussing multi-molecule entities such as dimers, clusters or crystals with multiple molecules per unit cell.

Table S1. Energy differences $\Delta E(\alpha-\beta)$ and $\Delta E(\gamma-\beta)$ between α-/γ-SA and β-SA calculated with six different exchange correlation functionals: the PBE[1] generalised-gradient approximation (GGA) exchange-correlation (XC) functional, the PBE0[2] and B3LYP[3] hybrid functionals, and PBE with the DFT-D2[4], DFT-D3[5] and Tkatchenko-Scheffler (DFT-TS)[6] dispersion corrections. The energy differences obtained with PBE-D2 and PBE-TS are compared to the calculations in Ref. 7. All energy differences are those obtained after full optimisation of the crystal structures.

XC	a [Å]	b [Å]	c [Å]	α [°]	β [°]	γ [°]	V [Å^3]	Δa [%]	Δb [%]	Δc[%]	$\Delta \alpha$ [%]	$\Delta \beta$ [%]	$\Delta \gamma$ [%]	ΔV[%]
Expt.	6.867	7.198	5.727	109.10	97.18	101.84	256	-	-	-	-	-	-	-
PBE	7.306	7.405	5.964	111.93	95.34	100.52	290	6.40	2.87	4.14	2.59	-1.89	-1.29	13.10
PBE0	7.135	7.333	5.897	111.56	95.63	100.96	277	3.90	1.88	2.97	2.25	-1.59	-0.86	8.13
B3LYP	7.301	7.457	5.989	112.11	95.09	100.14	293	6.32	3.59	4.58	2.76	-2.15	-1.67	14.42
PBE-D2	6.615	7.122	5.655	108.58	97.19	102.93	240	-3.67	-1.06	-1.26	-0.47	0.01	1.07	-6.09
PBE-D3	6.762	7.160	5.691	109.02	96.85	101.89	250	-1.53	-0.52	-0.63	-0.07	-0.34	0.05	-2.50
PBE-TS	6.785	7.147	5.690	108.89	96.95	101.99	250	-1.19	-0.71	-0.65	-0.19	-0.23	0.14	-2.37

Table S2. Optimised lattice parameters of α-SA obtained with the PBE, PBE0, B3LYP, PBE-D2, PBE-D3 and PBE-TS exchange-correlation functionals (XC). The experimental values are shown in the first row for comparison, and the rightmost columns show the percentage deviation between the calculations and these values.

XC	a [Å]	b [Å]	c [Å]	β [°]	V [Å^3]	Δa [%]	Δb [%]	Δc[%]	$\Delta \beta$ [%]	ΔV[%]
Expt.	5.464	8.766	5.004	93.29	239	-	-	-	-	-
PBE	5.754	9.183	5.396	85.83	284	5.31	4.76	7.84	-8.00	18.85
PBE0	5.619	9.034	5.221	88.29	265	2.84	3.06	4.34	-5.36	10.72
B3LYP	5.739	9.115	5.370	86.62	280	5.04	3.98	7.32	-7.15	17.20
PBE-D2	5.422	8.660	4.948	93.76	232	-0.78	-1.21	-1.13	0.51	-3.13
PBE-D3	5.477	8.754	5.033	92.28	241	0.23	-0.13	0.58	-1.09	0.76
PBE-TS	5.478	8.746	5.048	92.10	242	0.27	-0.23	0.88	-1.27	1.02

Table S3. Optimised lattice parameters of β-SA obtained with the PBE, PBE0, B3LYP, PBE-D2, PBE-D3 and PBE-TS exchange-correlation functionals (XC). The experimental values are shown in the first row for comparison, and the rightmost columns show the percentage deviation between the calculations and these values.

XC	a [Å]	b [Å]	c [Å]	β [°]	V [Å^3]	Δa [%]	Δb [%]	Δc[%]	$\Delta \beta$ [%]	ΔV[%]
Expt.	5.702	8.415	10.354	90.37	497	-	-	-	-	-
PBE	6.025	8.828	10.827	94.26	574	5.67	4.90	4.57	4.30	15.60
PBE0	5.838	8.766	10.609	92.97	542	2.40	4.17	2.47	2.88	9.16
B3LYP	5.954	8.911	10.811	93.99	572	4.43	5.88	4.42	4.00	15.18
PBE-D2	5.631	8.243	10.337	89.39	480	-1.24	-2.05	-0.16	-1.09	-3.42
PBE-D3	5.697	8.414	10.369	90.31	497	-0.09	-0.02	0.15	-0.07	0.04
PBE-TS	5.649	8.370	10.390	89.90	491	-0.92	-0.53	0.35	-0.53	-1.10

Table S4. Optimised lattice parameters of γ-SA obtained with the PBE, PBE0, B3LYP, PBE-D2, PBE-D3 and PBE-TS exchange-correlation functionals (XC). The experimental values are shown in the first row for comparison, and the rightmost columns show the percentage deviation between the calculations and these values.

	RMSD [10^{-2} Å]		
XC	**α-SA**	**β-SA**	**γ-SA**
PBE	-	-	-
PBE0	2.17	2.32	2.43
B3LYP	1.46	1.45	1.59
PBE-D2	1.12	1.22	2.63
PBE-D3	0.80	1.61	2.78
PBE-TS	0.83	1.61	2.46

Table S5. Root mean square distance (RMSD) between succinic acid (SA) molecules extracted from the α-SA, β-SA and γ-SA structures optimised with the PBE, PBE0, B3LYP, PBE-D2, PBE-D3 and PBE-TS exchange-correlation functionals (XC). The RMSD values in each column are calculated with respect to the PBE structures, and the statistical analyses were performed using the tools in the VMD software[8].

	***d*(C=O--H) [Å]**		
XC	**α-SA**	**β-SA**	**γ-SA**
PBE	1.566	1.589	1.591
PBE0	1.586	1.613	1.601
B3LYP	1.636	1.660	1.651
PBE-D2	1.538	1.573	1.552
PBE-D3	1.542	1.581	1.557
PBE-TS	1.537	1.577	1.553

Table S6. C=O…H H-bond distances in the succinic acid (SA) dimers in α-, β-, and γ-SA structures optimised with the PBE, PBE0, B3LYP, PBE-D2, PBE-D3 and PBE-TS exchange-correlation functionals (XC). The distances shown are averaged over all dimers in the unit cell and the standard deviations are on the order of 10^{-4}, 10^{-8} and 10^{-7} Å, respectively, for the α-, β-, and γ-SA structures.

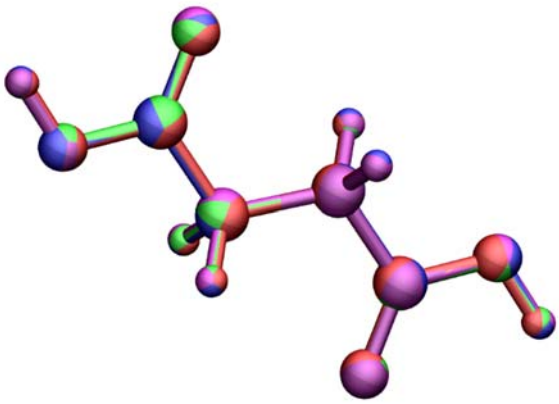

Figure S1. Overlay of the planar succinic acid (SA) molecules taken from α-SA structures optimised with the PBE (blue), PBE0 (red), B3LYP (green), PBE-D2 (purple), PBE-D3 (orange) and PBE-TS (magenta) functionals. The molecules were aligned and the image generated using VMD.

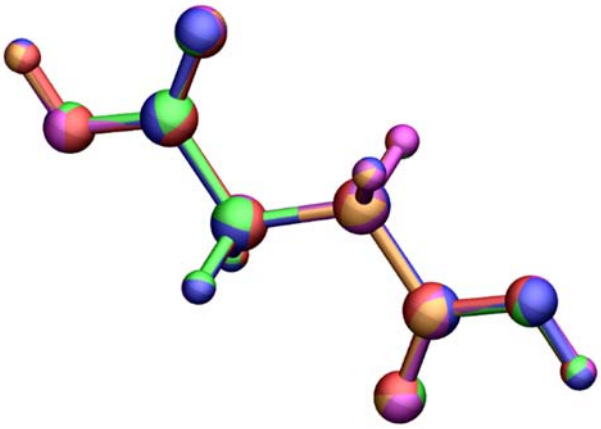

Figure S2. Overlay of the planar succinic acid (SA) molecules taken from β-SA structures optimised with the PBE (blue), PBE0 (red), B3LYP (green), PBE-D2 (purple), PBE-D3 (orange) and PBE-TS (magenta) functionals. The molecules were aligned and the image generated using VMD.

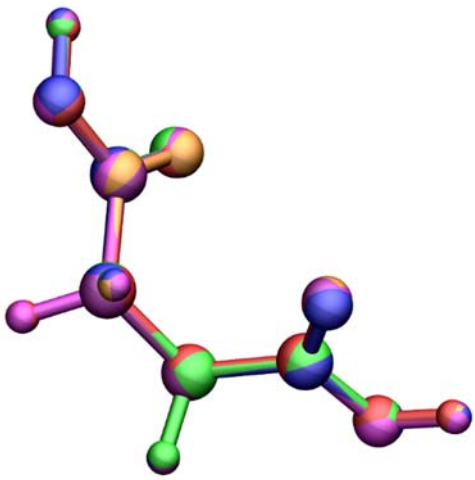

Figure S3. Overlay of the twisted succinic acid (SA) molecules taken from γ-SA structures optimised with the PBE (blue), PBE0 (red), B3LYP (green), PBE-D2 (purple), PBE-D3 (orange) and PBE-TS (magenta) functionals. The molecules were aligned and the image generated using VMD.

XC	ΔE(Twisted - Planar) [kJ mol^{-1} molec^{-1}]	
	Molecule	Dimer
PBE	-0.7	-1.1
PBE0	-1.0	-1.1
B3LYP	-0.7	-0.9
PBE-D2	-1.9	-2.6
PBE-D3	-1.4	-2.0
PBE-TS	-1.7	-2.3

Table S7. Differences in the gas-phase total energies of the twisted (γ) and planar (α/β) conformations of a single succinic acid molecule obtained using the PBE, PBE0, B3LYP, PBE-D2, PBE-D3 and PBE-TS exchange-correlation functionals.

XC	Dimer E_F [kJ mol^{-1}]		
	Planar	Twisted	ΔE_F (Twisted - Planar)
PBE	-73.4	-74.2	-0.8
PBE0	-71.1	-71.3	-0.2
B3LYP	-65.1	-65.5	-0.4
PBE-D2	-82.7	-83.9	-1.2
PBE-D3	-80.6	-81.9	-1.3
PBE-TS	-80.0	-81.3	-1.4

Table S8. Gas-phase dimer formation energies $E_F = E(Dimer) - 2E(Monomer)$ (i.e. H-bond formation energies) for the twisted (γ) and planar (α/β) conformations of succinic acid obtained using the PBE, PBE0, B3LYP, PBE-D2, PBE-D3 and PBE-TS exchange-correlation functionals (XC). The rightmost column shows the difference in the formation energies of the twisted and planar dimers.

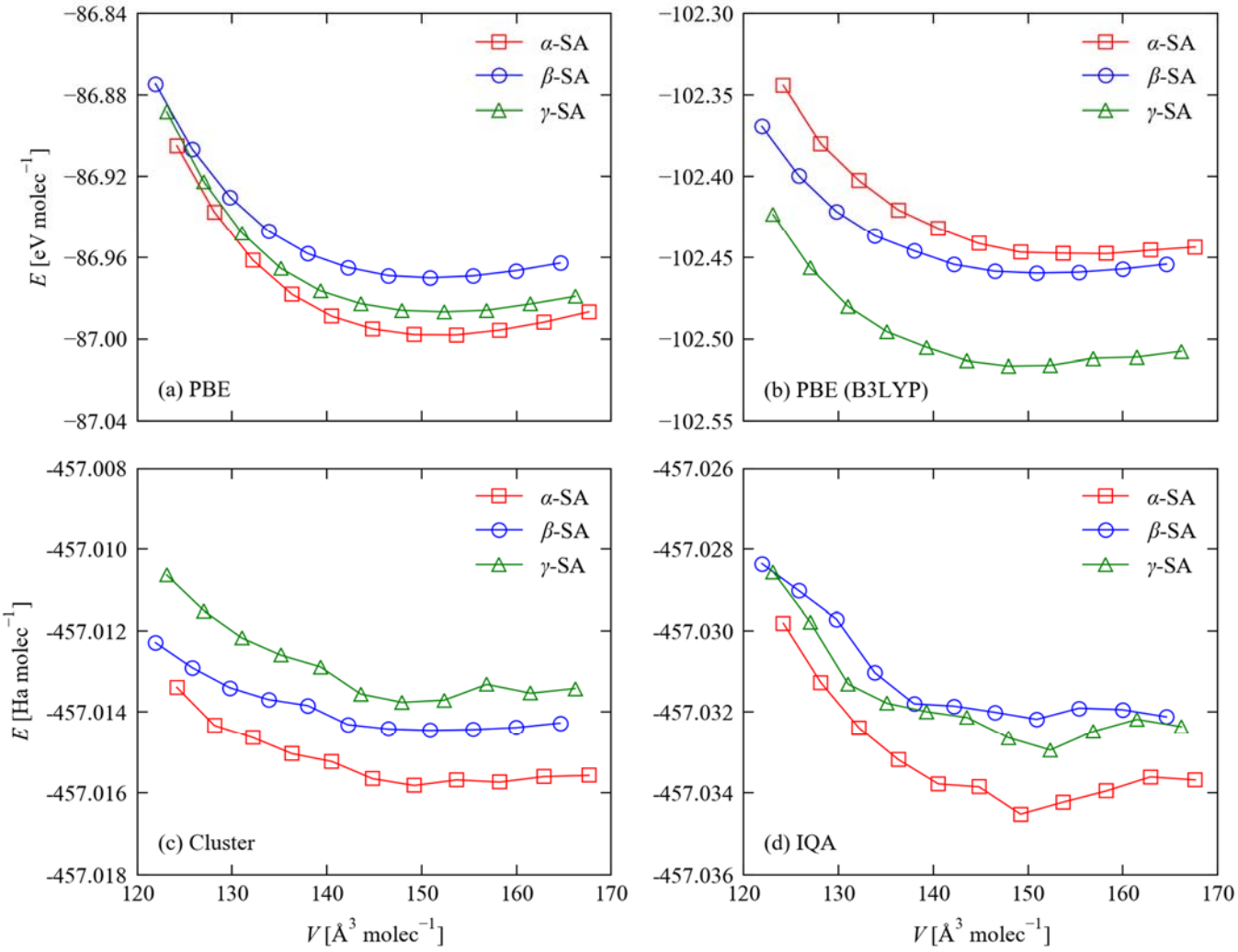

Figure S4. Comparison of energy/volume curves for α-SA (red squares), β-SA (blue circles) and γ-SA (green triangles) calculated using four methods: (a) constant-volume geometry optimisation with the PBE exchange-correlation functional, (b) single-point B3LYP calculations on the PBE-optimised structures, (c) single-point B3LYP calculations on gas-phase cluster models extracted from the PBE-optimised structures, and (d) partitioned IQA energies[9] from reference central molecules in the clusters. These plots clearly show the energetic stability ordering predicted by the different methods.

V [Å^3 molec^{-1}]	RMSD [10^{-3} Å]	φ [°]	d_{HB} [Å]	Δd_{HB} [10^{-2} Å]
124	9.30	180	1.521	-4.55
128	6.97	180	1.536	-3.08
132	4.84	180	1.538	-2.80
136	3.15	180	1.547	-1.98
141	2.34	180	1.551	-1.50
145	-	180	1.566	-
149	1.58	180	1.574	0.78
154	3.38	180	1.573	0.63
158	4.55	180	1.579	1.30
163	6.01	180	1.580	1.34
168	7.62	180	1.584	1.75

Table S9. Structural changes in the succinic acid monomer geometry and dimer H-bonding distance d_{HB} in α-SA as a function of volume compressions and expansions about the optimised equilibrium obtained using the PBE functional. The RMSD values in the second column are calculated with respect to the monomer geometry at the equilibrium volume using the VMD software, and the φ angle in the third column is the C-C-C-C dihedral angle defined in Fig. 2 in the main text.

V [Å^3 molec^{-1}]	RMSD [10^{-3} Å]	φ [°]	d_{HB} [Å]	Δd_{HB} [10^{-2} Å]
122	6.81	180	1.559	-3.07
126	5.28	180	1.564	-2.48
130	3.93	180	1.570	-1.90
134	3.15	180	1.572	-1.69
138	2.91	180	1.573	-1.64
142	-	180	1.589	-
147	1.59	180	1.591	0.18
151	2.03	180	1.593	0.38
155	2.49	180	1.594	0.46
160	3.00	180	1.594	0.48
165	3.74	180	1.592	0.31

Table S10. Structural changes in the succinic acid monomer geometry and dimer H-bonding distance d_{HB} in β-SA as a function of volume compressions and expansions about the optimised equilibrium obtained using the PBE functional. The RMSD values in the second column are calculated with respect to the monomer geometry at the equilibrium volume using the VMD software, and the φ angle in the third column is the C-C-C-C dihedral angle defined in Fig. 2 in the main text.

V [Å^3 molec^{-1}]	RMSD [10^{-3} Å]	φ [°]	d_{HB} [Å]	Δd_{HB} [10^{-2} Å]
123	25.4	77.36	1.533	-5.73
127	20.3	77.41	1.543	-4.72
131	15.0	77.42	1.554	-3.70
135	10.3	77.38	1.561	-2.93
139	5.71	77.38	1.567	-2.32
144	-	77.46	1.591	-
148	4.38	77.54	1.598	0.72
152	8.38	77.53	1.599	0.88
157	13.6	77.30	1.587	-0.37
161	16.5	77.36	1.600	0.90
166	20.6	77.29	1.600	0.93

Table S11. Structural changes in the succinic acid monomer geometry and dimer H-bonding distance d_{HB} in γ-SA as a function of volume compressions and expansions about the optimised equilibrium obtained using the PBE functional. The RMSD values in the second column are calculated with respect to the monomer geometry at the equilibrium volume using the VMD software, and the φ angle in the third column is the C-C-C-C dihedral angle defined in Fig. 2 in the main text.

References

(1) Perdew, J. P.; Burke, K.; Ernzerhof, M. Generalized Gradient Approximation Made Simple. *Phys. Rev. Lett.* **1996**, *77*, 3865. https://doi.org/10.1103/PhysRevLett.77.3865.

(2) Adamo, C.; Barone, V. Toward Reliable Density Functional Methods without Adjustable Parameters: The PBE0 Model. *J. Chem. Phys.* **1999**, *110*, 6158. https://doi.org/10.1063/1.478522.

(3) Becke, A. D. A New Mixing of Hartree-Fock and Local Density-Functional Theories. *J. Chem. Phys.* **1993**, *98*, 1372. https://doi.org/10.1063/1.464304.

(4) Grimme, S. Semiempirical GGA-Type Density Functional Constructed with a Long-Range Dispersion Correction. *J. Comput. Chem.* **2006**, *27*, 1787. https://doi.org/10.1002/jcc.20495.

(5) Grimme, S.; Antony, J.; Ehrlich, S.; Krieg, H. A Consistent and Accurate Ab Initio Parametrization of Density Functional Dispersion Correction (DFT-D) for the 94 Elements H-Pu. *J. Chem. Phys.* **2010**, *132*, 154104. https://doi.org/10.1063/1.3382344.

(6) Tkatchenko, A.; Scheffler, M. Accurate Molecular van der Waals Interactions from Ground-State Electron Density and Free-Atom Reference Data. *Phys. Rev. Lett.* **2009**, *102*, 073005. https://doi.org/10.1103/PhysRevLett.102.073005.

(7) Lucaioli, P.; Nauha, E.; Gimondi, I.; Price, L. S.; Guo, R.; Iuzzolino, L.; Singh, I.; Salvalaglio, M.; Price, S. L.; Blagden, N. Serendipitous Isolation of a Disappearing Conformational Polymorph of Succinic Acid Challenges Computational Polymorph Prediction. *CrystEngComm* **2018**, *20*, 3971. https://doi.org/10.1039/C8CE00625C.

(8) Humphrey, W.; Dalke, A.; Schulten, K. VMD: Visual Molecular Dynamics. *J. Mol. Graph.* **1996**, *14*, 33. https://doi.org/10.1016/0263-7855(96)00018-5.

(9) Blanco, M. A.; Martín Pendás, Á.; Francisco, E. Interacting Quantum Atoms: A Correlated Energy Decomposition Scheme Based on the Quantum Theory of Atoms in Molecules. *J. Chem. Theory Comput.* **2005**, *1*, 1096. https://doi.org/10.1021/ct0501093.